

**Enhancing the antimicrobial and antibiofilm effectiveness of silver nanoparticles prepared by green synthesis**

Journal:	<i>Journal of Materials Chemistry B</i>
Manuscript ID	TB-ART-04-2018-000907.R1
Article Type:	Paper
Date Submitted by the Author:	14-May-2018
Complete List of Authors:	Oliver, Susan; University of New South Wales, Centre Advances MAcromolecular Design Wagh, Harsha ; University of New South Wales, Centre Advances MAcromolecular Design Liang, Yuanli ; University of New South Wales, Centre Advances MAcromolecular Design Yang, Shuang ; University of New South Wales, Centre Advances MAcromolecular Design Boyer, Cyrille; University of New South Wales, Centre Advances MAcromolecular Design

Enhancing the antimicrobial and antibiofilm effectiveness of silver nanoparticles prepared by green synthesis

Susan Oliver,^{a,b} Harsha Wagh,^b Yuanli Liang,^b Shuang Yang,^b and Cyrille Boyer^{a,b*}

^a*Australian Centre for NanoMedicine (ACN), School of Chemical Engineering, University of New South Wales, Sydney, Australia 2052.*

^b*Centre for Advanced Macromolecular Design (CAMD), School of Chemical Engineering, University of New South Wales, Sydney, Australia 2052.*

Abstract

The use of polyphenol-rich plant extracts is well established for the green synthesis of silver nanoparticles (AgNPs). However, the size of the AgNPs varies substantially depending on the extract used and many researchers report sizes above 20 nm, which are not optimal for antimicrobial activity. Herein, using catechin as a model polyphenol, we have explored two techniques to improve its stabilising capacity and therefore decrease the subsequent AgNP size: cross-linking catechin with sodium tetraborate (borax); and preparation of a water soluble oligomer from catechin (polycat). The prepared AgNPs from the three stabilising systems, cat@AgNPs, cat-borax@AgNPs and polycat@AgNPs, were characterised by UV-Vis spectroscopy, dynamic light scattering (DLS), X-Ray diffraction (XRD), transmission electron microscopy (TEM) and inductively coupled plasma mass spectrometry (ICP-MS). Cat-borax produced smaller AgNPs (18.4 nm) than catechin (42.3 nm) but the smallest particles were prepared with polycat (8.5 nm). Antimicrobial efficacy was assessed against gram positive and gram negative bacteria and was compared with 10 nm sodium citrate capped AgNPs (citrate@AgNPs). Polycat@AgNPs showed superior antimicrobial inhibitory to cat@AgNPs and cat-borax@AgNPs as well as citrate@AgNPs, exhibiting MICs of only 1.25 µg/mL (Ag) for *Pseudomonas aeruginosa*

and *Acinetobacter baumannii*. Polycat@AgNPs also demonstrated substantially enhanced antibiofilm activity. An Ag concentration of only 5 $\mu\text{g/mL}$, was sufficient for a 99.9% reduction in biofilm cell viability and a 99.1% reduction in biofilm biomass with polycat@AgNPs. Uptake of polycat@AgNPs by bacteria was determined to be significantly higher than for citrate@AgNPs and tomographic and SEM images showed evidence of destruction of bacteria cells by polycat@AgNPs.

Introduction

Bacterial infections are a growing health concern and a major cause of deaths worldwide.¹⁻⁴ Of particular concern, are pathogens embedded in biofilms, self-produced polymer matrices comprising polysaccharide, protein and DNA, which can protect bacteria against antimicrobial agents.^{5,6} Biofilms can form on both living tissues and abiotic surfaces and are typically more difficult to kill than planktonic bacteria thereby causing chronic infections.^{5,6}

The antimicrobial properties of silver have been known since at least the 8th century and silver nanoparticles (AgNPs) are well-established as potent antimicrobial agents.⁷⁻⁹ AgNPs have also demonstrated some potential in the inhibition and eradication of biofilms,¹⁰⁻¹² however, biofilm cells are up to 25 times more resistant to AgNPs than planktonic cells.¹³

Much work has been done on the elucidation of the mechanism of action of AgNPs,^{7,9,14-16} however, the exact mechanism of action remains somewhat elusive.¹⁷ The antimicrobial activity of AgNPs is multifaceted and mechanisms include: damage to cell membranes leading to increased permeability;^{18,19} generation of reactive oxygen species (ROS); DNA damage from AgNPs that penetrate the cell;²⁰ and release of antimicrobial silver ions.²¹⁻²³ AgNPs have also been shown to work synergistically with other antimicrobial agents.²⁴⁻²⁸

Traditionally AgNPs have been prepared by physical and chemical means but, more recently, green synthesis methods, including the use of plant extracts, biodegradable polymers and enzymes/bacteria,²⁹⁻³¹ have emerged as environmentally friendly alternatives.

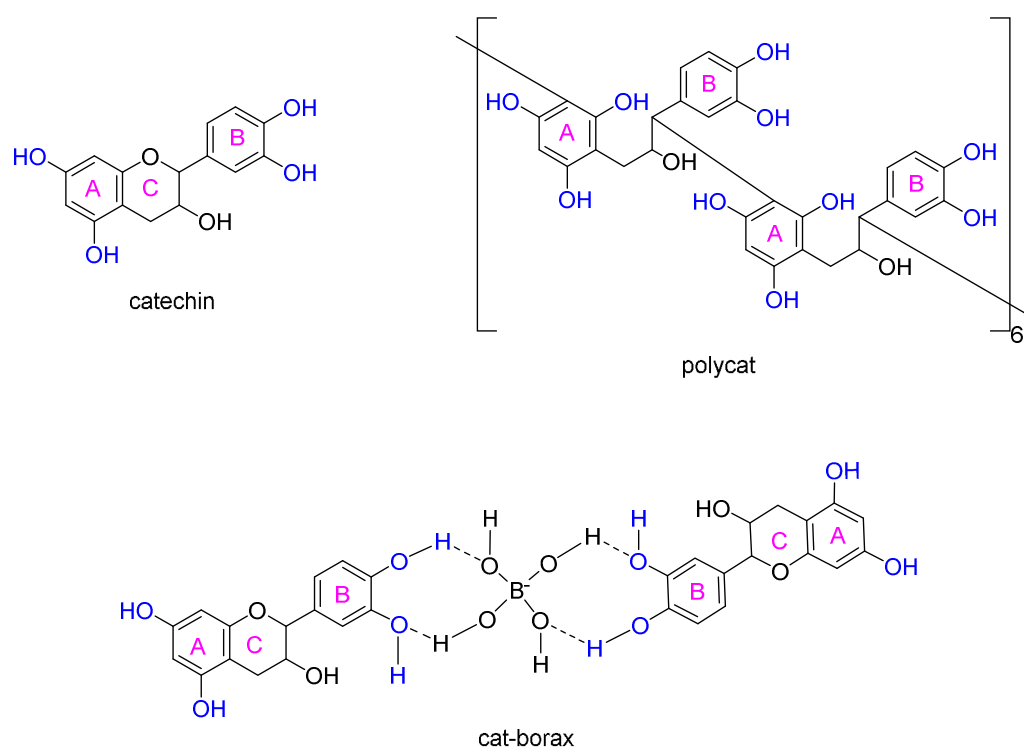
A large number of plant extracts have been used to prepare AgNPs³²⁻³⁴ and flavonoids and other polyphenols are often indicated as active ingredients, serving as both reducing and capping agents.³⁵⁻⁵⁹ Purified polyphenols have also been used.^{38,}

⁶⁰⁻⁶⁴ However, the size of the AgNPs varies substantially depending on the extract used⁶⁵ and many researchers report sizes above 20 nm,^{36-40, 42-48, 59, 60} which are not optimal for antimicrobial activity.⁶¹ AgNPs with sizes greater than 20 nm rely primarily on release of silver ions for antimicrobial efficacy²² whereas smaller AgNPs, in particular those 10 nm and below, are able to interact directly with bacteria.²⁰ The final size of metal nanoparticles is dependent on a number of factors, including the reaction rate and the effectiveness of stabilisers. For instance, small nanoparticles are produced with a fast nucleation rate, moderate crystal growth rate^{66, 67} and an effective stabiliser.^{68, 69} Using catechin as a model polyphenol, herein, we have explored how it can be modified to improve its stabilising capacity and thereby how the antimicrobial and antibiofilm efficacy of AgNPs prepared from catechin can be enhanced whilst maximising adherence to green principles, including the use of renewable materials and minimal energy usage.⁷⁰

Catechins, present in red wine, red berries, and green tea, are widely occurring members of the flavonoid group of polyphenols,⁷¹ which have demonstrated a number of therapeutic benefits, including mild antimicrobial activity.⁷²⁻⁷⁴ Green tea extract, an abundant source of catechins, has been used as reducing and capping agent in the preparation of AgNPs but the subsequent nanoparticles only had limited antimicrobial activity compared with those that were chemically prepared and polymer stabilised.⁴⁰ AgNPs prepared with pure catechin also displayed only modest antimicrobial activity.⁶⁰

Capping agents can either stabilise nanoparticles electrostatically or sterically.⁶⁹ Generally, the most effective capping agents will provide both steric and electrostatic stabilisation.⁷⁵ To effectively stabilise nanoparticles electrostatically a zeta-potential either above +30 mV or below -30 mV is recommended. AgNPs prepared from catechin meet this criterion but do not possess any additional steric stabilisation. We have investigated two techniques to improve the stabilising capacity of catechin and therefore decrease the subsequent AgNP size (see **Scheme 1** for structures of each

stabilising agent): cross-linking catechin with sodium tetraborate (borax); and preparation of a water soluble oligomer from catechin (polycat), which, in addition to electrostatic stabilisation, also provide steric stabilisation, and have compared their effectiveness with catechin. The same concentration of catechin (1 mM) and AgNO_3 (0.5 mM) was used for all three stabilising systems but other parameters, including pH (6, 7, 8, 9) and reaction conditions (room temperature vs. microwave assisted), were investigated to optimise AgNPs prepared with each stabilising system.



Scheme 1: Representative structures of the three stabilisers (catechin, cat-borax and polycat) explored for the in-situ synthesis of AgNPs.

Finally, antimicrobial efficacy of AgNPs prepared with each stabilising system was assessed against gram positive and gram negative bacteria as well as biofilms and was compared with 10 nm commercially available sodium citrate capped AgNPs.

Materials and methods

Materials: (+)-Catechin hydrate, 2,2-diphenyl-1-picrylhydrazyl (DPPH•), ethanol, hydrochloric acid (HCl), sodium carbonate (Na_2CO_3), sodium tetraborate (borax), silver nitrate (AgNO_3), 10 nm sodium citrate capped AgNPs and sodium hydroxide were purchased from Sigma Aldrich. Deionised (DI) water was produced by a Milli-Q water purification system and had a resistivity of 17.9 $\text{m}\Omega/\text{cm}$. Snakeskin dialysis tubing (MWCO-3500 g/mol) was purchased from ThermoFisher.

Polymerisation of catechin (polycat): Using a slight modification of the procedure previously developed by our group,⁷⁶ 500 mg of catechin was dissolved in 5 mL of ethanol and 5 mL HCl (final concentration 1 M HCl), protected from light and stirred for 48 h at 40 °C. The solution was neutralised with sodium hydroxide and then dialysed (MWCO-3500) for 5 days in the dark against ethanol/DI water then DI water (16 changes of solvent in total) and then lyophilised. UV-Vis spectroscopy was used to confirm the absence of catechin in the final dialysis water. Yield was 49%. Molecular weight (M_n) was measured by size exclusion chromatography (SEC) as previously described⁷⁶ using a calibration curve developed by identifying catechin monomers, dimers, trimers and tetramers and was found to be 3600 g/mol with a dispersity of 1.4. The polymers were stored at 4 °C protected from light until required.

Preparation of silver nanoparticles (AgNPs) from catechin/polycat: AgNPs were prepared either at room temperature or microwave assisted. For room temperature preparation, 0.25 mL of 10 mM AgNO_3 solution was added to 4.45 to 4.75 mL of catechin or polycat solution such that the concentration in the final 5 mL solution was 0.5 mM AgNO_3 and 1 mM catechin/polycat. The solution was adjusted to the desired pH with 0.01 M Na_2CO_3 (0, 0.05, 0.1 & 0.3 mL for pH 6, 7, 8 & 9, respectively) or to the desired borax concentration with 0.1 M borax. The solutions were then allowed to stand in the dark for a minimum of 24 h prior to use. For microwave assisted preparation, 5 mL of solution was prepared at 4 °C in a 25 mL vial, sealed

and then heated for 10 s at full power in an 1100 watt domestic microwave oven, followed by standing for 2 h at room temperature in the dark. ICP-MS was used to determine conversion of AgNO_3 to AgNPs. As-prepared samples were filtered through an ultracentrifuge tube (MWCO-3000g/mol) and the silver content of the filtrate was analysed by ICP-MS. Conversion of Ag^+ to AgNPs was greater than 99.99% for the optimal versions of all three formulations therefore the concentration of AgNPs in solution was equivalent to the initial AgNO_3 solution. As all reagents were benign, no purification was required prior to use.

Free radical scavenging ability: Using a slight modification of the procedure described by Qiao et al.,⁷⁷ 1 mL of 400 μM DPPH• in ethanol was added to 3 mL of ethanolic cat@AgNPs, cat-borax@AgNPs or polycat@AgNPs solution containing 1×10^{-7} moles of catechin. The solution was shaken and then stored in the dark for 30 min. The absorbance of the final solution was measured at 517 nm against an ethanol blank. Free radical scavenging activity was calculated using the following equation:

$$\% \text{ Inhibition} = [\text{A}_\text{C} - (\text{A}_\text{S} - \text{A}_\text{N})] / \text{A}_\text{C} \times 100 \quad \text{Equation 1}$$

where A_C is the absorbance of the control (ethanol instead of AgNP solution), A_S is the absorbance of the tested sample and A_N is the absorbance of the sample with ethanol instead of DPPH• solution. All assays were undertaken in triplicate.

Minimum inhibitory concentration (MIC) determination: The MIC was determined for four bacterial strains - *Escherichia coli* K12, *Pseudomonas aeruginosa* PAO1, *Acinetobacter baumannii* ATCC 1906 and *Staphylococcus aureus* ATCC 29213 using the broth microdilution method in accordance with the Clinical and Laboratory Standards Institute (CLSI) guidelines. Bacterial culture was grown overnight from a single colony in 10 mL of Mueller-Hinton broth (MHB) at 37 °C with shaking at 180 rpm. A subculture was prepared from the overnight culture by diluting 50 μL in 5 mL MHB and growing to mid-log phase (approximately 2.5 h), then diluted to ca. 1×10^6 cells per mL. A two-fold dilution series of 50 μL of AgNPs

in MHB solution were added to a 96-well microplate followed by the addition of 50 μL of the subculture suspension. (Concentrations of AgNPs tested were 20, 10, 5, 2.5, 1.25 and 0.63 $\mu\text{g}/\text{mL}$.) The final concentration of bacteria in each well was ca. 5×10^5 cells per mL. As AgNPs are coloured, a dilution series without the addition of bacteria was prepared as a negative control. Positive controls without AgNPs and negative controls without bacteria or AgNPs were also included. The plates were then incubated at 37 °C for 20 h to ensure sufficient growth of inhibited bacteria, and the absorbance at 595 nm was measured with a microtiter plate reader (FLUOstar Omega, BMG Labtech). Bacterial growth inhibition was calculated using the following equation:

$$\% \text{ Inhibition} = [1 - ((A_{\text{CP}} - A_{\text{CN}}) - (A_{\text{SB}} - A_{\text{SC}})) / (A_{\text{CP}} - A_{\text{CN}})] \times 100 \quad \text{Equation 2}$$

where A_{CP} is the absorbance of the positive control (no AgNP solution), A_{CN} is the absorbance of the negative control (MHB only), A_{SB} is the absorbance of the tested sample and A_{SC} is the absorbance of the sample with MHB instead of bacteria. MIC values were defined as the lowest concentration of the sample that showed no visible growth and inhibited cell growth by more than 90%. All assays included three replicates and were repeated in at least three independent experiments.

Bacteria killing assessment: The bactericidal properties of the AgNPs were assessed against planktonic and biofilm bacteria using *P. aeruginosa* PAO1 in accordance with the method previously described by our group.⁷⁸ *P. aeruginosa* was grown overnight from a single colony in 10 mL of Luria Bertani medium (LB 10) at 37 °C with shaking at 180 rpm. The overnight culture was diluted 1 : 100 in M9 complete medium and 1 mL per well was added to tissue-culture treated 24-well plates (Costar, Corning®). The plates were incubated at 37 °C with shaking at 180 rpm for 6 h. AgNPs (or DI water for control) were then added to the wells to achieve a concentration of 5 $\mu\text{g}/\text{mL}$ and the plates were incubated for 60 min with shaking. After treatment, planktonic and biofilm viability was determined by a drop plate method. For planktonic analysis, free-floating cells in the biofilm supernatant were

serially diluted in sterile PBS and plated onto LB-10 agar. Images of undiluted planktonic bacteria were captured with a tomographic microscope (3D Cell Explorer, NanoLive, Lausanne, Switzerland). For biofilm analysis, cells attached to the interior surfaces of the well (surface area 4.5 cm²) were washed twice with sterile PBS to remove loosely attached bacteria, before being resuspended and homogenised in 1 mL PBS by incubating in an ultrasonication bath (150 W, 40 kHz; Unisonics, Australia) for 20 min and then serially diluted and plated onto LB-10 agar. Planktonic and biofilm colonies were counted after 24 h incubation at 37 °C. All assays included two replicates and were repeated in at least three independent experiments.

Biofilm dispersal assessment: *P. aeruginosa* biofilms were grown from 2 mL of subculture on 35 mm tissue culture dishes (FluoroDish, World Precision Instruments Inc., Sarasota, FL, USA) as described in the bacteria killing assessment. AgNPs (or DI water for control) were then added to the dishes to achieve a concentration of 5 µg/mL and the dishes were incubated for 60 min with shaking. After treatment, the supernatant was removed and the biofilm attached to the surface was washed twice with 2 mL of PBS, followed by the addition of 1 mL PBS. Images were then captured from at least eight different regions of the dishes with a 3D tomographic microscope (3D Cell Explorer, NanoLive, Lausanne, Switzerland) and the biofilm volume was determined with Steve digital staining software. All assays were repeated in at least two independent experiments.

Silver ion release assessment: 5 µg/mL of AgNPs were added to M9 complete medium and incubated at 37 °C with shaking at 180 rpm for 60 min. The solutions were then filtered through an ultracentrifuge tube (MWCO-3000g/mol) and the silver content of the filtrate was analysed by ICP-MS. All assays were performed in triplicate.

AgNP uptake by bacteria: *P. aeruginosa* bacteria were grown and treated as described in the bacteria killing assessment and were then centrifuged at 4000 rpm for 10 min and washed 3 times with DI water. The bacteria were then digested overnight at 70 °C in 70% nitric acid. The samples were diluted with DI water and the silver content of the solution was analysed by ICP-MS. AgNPs in M9 complete medium without bacteria were also centrifuged as controls and no precipitation occurred. All assays were performed in triplicate.

Statistical analysis: Statistical analyses were performed with GraphPad Prism 7 (GraphPad Software) using two-way ANOVA followed by Tukey's multiple comparisons test comparing treatments with control as well as comparing between treatments. Data is presented as mean \pm SD.

Analytical instruments

¹H-NMR Spectroscopy. All experiments were performed on a Bruker Avance 500 MHz NMR spectrometer, equipped with a 5mm TBI probe. All experiments were run with a gas flow across the probes of 535 L/h, with sample spinning, and at a temperature of 25 °C. Samples were dissolved in deuterated NMR solvents supplied by Cambridge Isotopes (15% DMSO-*d*₆ / 85% D₂O). Spectra were referenced to residual protons in the NMR solvent (DMSO-*d*₆: δ 2.60). A presaturation water suppression experiment was employed to eliminate the residual non deuterated signal from the solvent.⁷⁹ Diffusion Ordered Spectroscopy (DOSY) was performed using a stimulated echo pulse program, which included bi-polar gradients and a watergate element for water suppression.⁸⁰ A linear sequence of 16 steps with gradient strengths from 2% to 95%, where the gradient is 50 G/cm, was used.

UV Vis Spectroscopy. UV-Vis spectra were recorded in a 1 cm disposable cuvette against DI water using a CARY 3000 spectrometer from Varian at 25 °C. All samples were diluted 4-fold with DI water.

Dynamic light scattering (DLS): DLS was carried out on a Malvern Zetasizer Nano Series running DTS software (He-Ne laser, 4 mW, $\lambda = 633 \text{ nm}$, angle 173°). For size measurements 100 μL of as prepared AgNP solutions were diluted in 1 mL of DI water whereas zeta potentials were determined on undiluted AgNP solutions.

Inductively coupled plasma mass spectrometry (ICP-MS): ICP-MS was performed on aqueous samples acidified with HNO_3 by a PerkinElmer quadrupole Nexion ICP-MS.

Oxidation/reduction potential (ORP) and pH measurements: ORP was measured with pH/ORP/ISE meter from Hanna Instruments (HI 98191) equipped with a gel filled PEI body ORP electrode. pH was measured with a SevenCompact™ pH/Ion meter from Mettler Toledo.

X-Ray Diffraction (XRD). XRD was performed on a PANalytical Empyrean thin film diffractometer over a 2θ range of 30 to 80° with a step size of 0.026° and a scan step time of 116.79s. Samples were prepared as thin films with several drops of as prepared AgNPs added to glass slides and allowed to air dry between drops. The glass slides were then heated overnight in an oven at 90°C prior to analysis. Spectra were processed using Highscore Plus software and crystallite size was determined using the Scherrer equation.

Transmission Electron Microscopy (TEM): TEM images of AgNPs were captured using a JOEL-1400 microscope with an accelerating voltage of 100 kV. 10 μL of as-prepared AgNP solution was drop cast onto carbon coated copper grids and allowed to air dry for 24 h prior to analysis. Size distribution was determined by measuring a minimum of 200 particles using Image-J software.

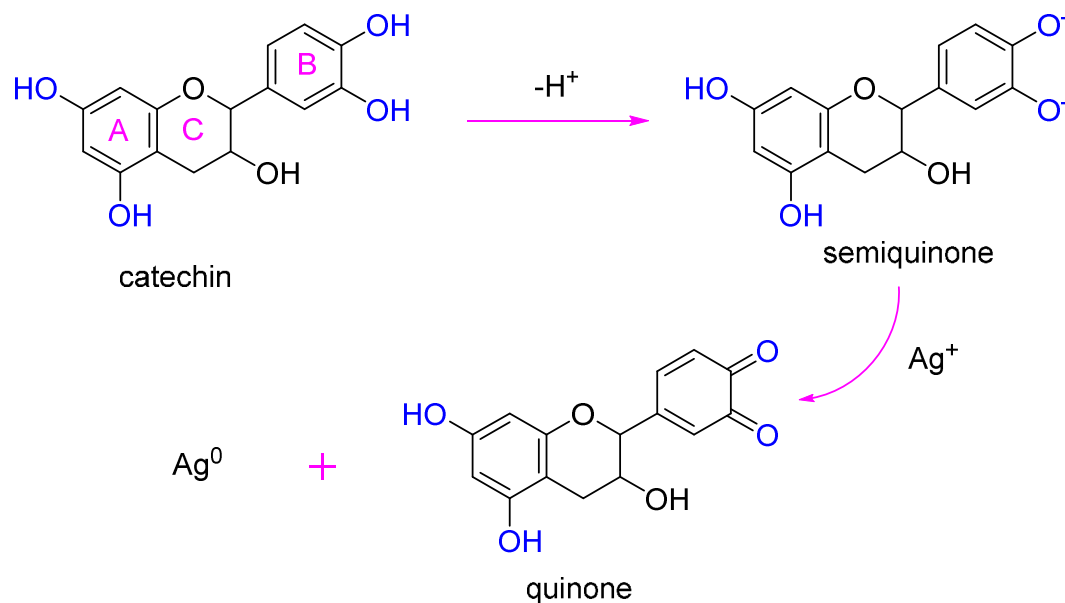
Field-Emission Scanning Electron Microscopy (FE-SEM): SEM images of *P. aeruginosa* bacteria were captured using a FEI Nova NanoSEM 450 FE-SEM operating in immersion mode with a voltage of 5 kV. Bacteria were grown and treated as described in the bacteria killing assessment and were then centrifuged at 4000 rpm

for 10 min. The supernatant was discarded and the bacteria were fixed with 2.5% glutaraldehyde in 0.1 M sodium cacodylate buffer for 60 min and then washed with 0.1 M sodium cacodylate buffer. The bacteria were then added to poly-L-lysine coated glass coverslips and, after 5 min, washed 3 times with DI water then post-fixed in a microwave with 1% OsO₄ in 0.1 M Sodium cacodylate buffer. The coverslips were then washed again with DI water followed by a series of microwave assisted ethanol dehydration steps (30%, 50%, 70%, 90%, 100%, 100% ethanol). After critical point drying in CO₂, the coverslips were mounted on stubs with carbon tape and sputter coated with platinum.

Results and discussion:

Synthesis of silver nanoparticles

AgNPs are often characterised by identification of their surface plasmon resonance (SPR) by UV-Vis absorption.⁸¹ SPR peaks typically occur between 390 and 530 nm and can be correlated with the size of the AgNPs.⁸¹ Smaller nanoparticles typically show an SPR peak at shorter wavelengths⁸² but this may be red-shifted in the presence of a capping agent.⁸³⁻⁸⁶ In characterising nanoparticles prepared using polyphenols, it is also important to consider that catechol groups are oxidised to quinones in the process (see **Scheme 2** for example with catechin) and quinones typically exhibit UV-Vis absorption^{87, 88} in the same region as the SPR band of AgNPs. We have therefore overlaid the UV-Vis spectra of pure oxidised catechin and polycat with the UV-Vis spectra of AgNPs prepared with catechin, cat-borax and polycat (**Figure 1**) for easy evaluation.



Scheme 2: Reduction of silver nitrate to silver nanoparticles by catechin

Catechin as reducing and capping agent

Figure 1a and b show the effect of varying pH on the appearance and UV-Vis absorbance of AgNP solutions prepared by catechin at room temperature and with microwave assistance, respectively. As can be seen, in general, the absorption peak increases and shifts to a lower wavelength with increasing pH and solutions show a deepening in colour, suggesting smaller AgNPs have been prepared at higher pHs. Indeed, at lower pHs, the SPR peak cannot be distinguished from the absorbance of oxidised catechin. These results accord with the measured standard reduction potentials of catechin, which were 390, 334, 262 and 213 mV at pH 6, 7, 8 and 9, respectively. An increase in reduction potential at low pH favours a decrease in the reduction reaction rate and therefore the nucleation rate, resulting in the formation of larger sized particles. Furthermore, higher pHs can reduce Ag^+ to Ag^0 via an $Ag(OH)_x$ intermediate, which also increases the nucleation rate.⁸⁹

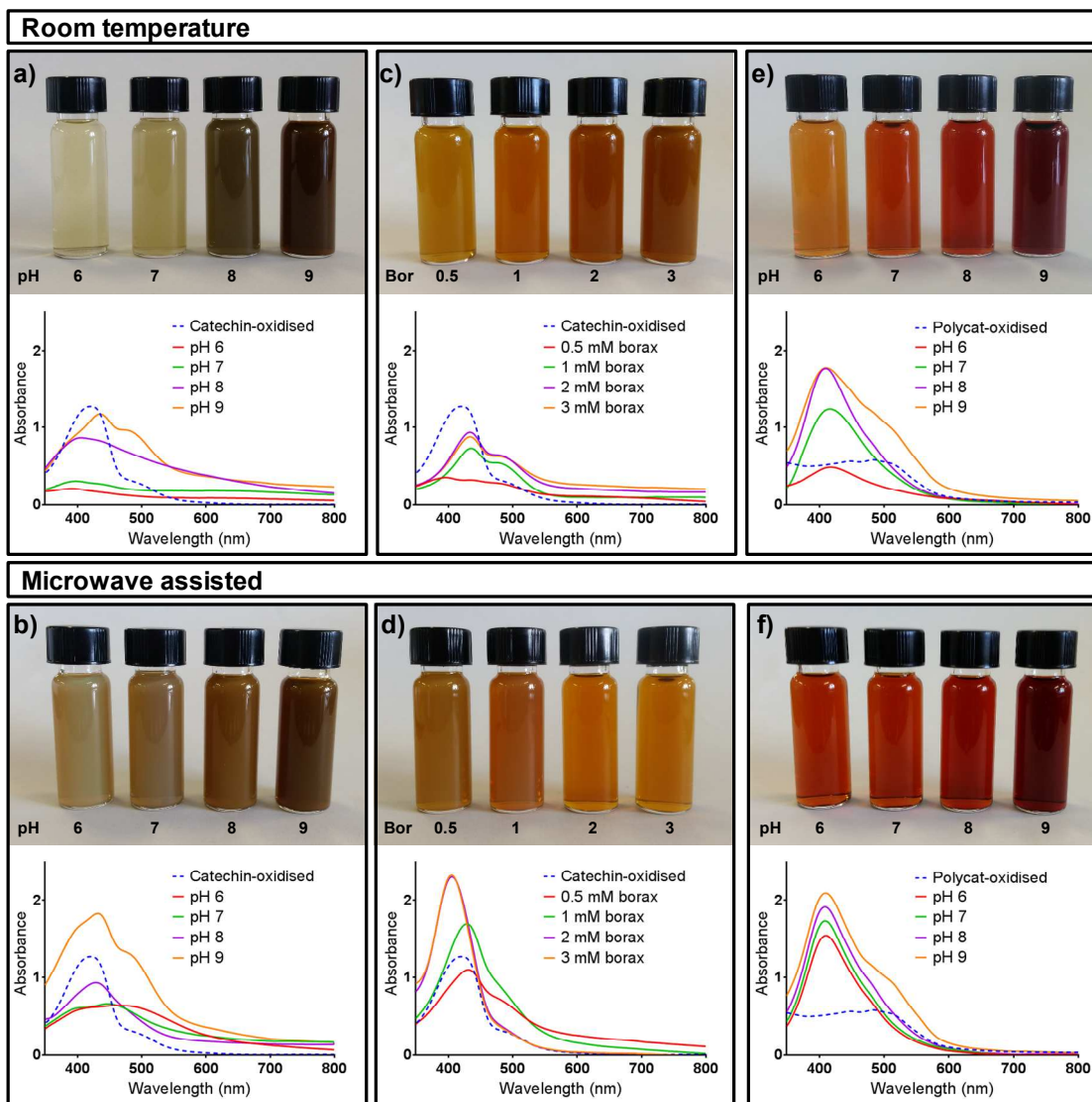


Figure 1: Digital photographs and UV-Vis spectra showing the effect of varying reaction parameters for AgNPs prepared with catechin (a,b); cat-borax (c,d) and polycat (e,f). All samples were diluted 4-fold with DI water prior to UV-Vis spectroscopy therefore the Ag concentration was 0.125mM for all spectra.

A number of researchers have used microwave irradiation to facilitate the production of AgNPs,^{57, 90-95} however, it doesn't always lead to smaller particle size.⁹⁶ We used a domestic microwave to investigate the effect of microwave radiation on particle size. Different reaction times were explored and 10 secs (for a 5 mL sample)

was found to be optimal for minimising particle size (data not shown). We believe this short reaction time maximised nucleation whilst minimising aggregation during the microwave treatment. For AgNPs prepared by catechin at pH 9, an immediate colour change was noted at room temperature, indicating that rapid nucleation was already occurring. In this case (pH 9.0), microwaving did not lead to smaller particle sizes as evidenced by no reduction observed in the SPR wavelength (see **Figure 1b** and **Table 1**). Furthermore, DLS measurements (**Table 1**) suggested the presence of some larger particles, possibly from an increase in oxidised product from the elevated temperature. On the other hand, for reactions that proceeded more slowly at room temperature (pH ≤ 8) microwaving increased the nucleation rate and therefore led to smaller particles.

For microwave assisted AgNPs, increasing the pH from 8 to 9 led to an increase in the height of the SPR peak but there was no further decrease in its wavelength. It is also apparent from the shape of the UV-Vis spectrum that considerable oxidation of catechin occurred. Furthermore, both the number average and volume average particle sizes are smaller for those prepared at pH 8 vs. pH 9 (53 & 128 vs 108.0 & 153.2 nm, respectively) and no significant difference is seen in the intensity average (**Table 1**). The ability of capping agents to stabilise NPs is highly dependent on the capping agent's solubility.⁶⁹ When oxidised, the catechol groups on catechin are replaced by quinones (see **Scheme 2**), which are significantly less soluble in water.⁸⁷ Hence, if excessive oxidation occurs, the stabilising capacity of catechin is reduced and this favours aggregation. Although some oxidation of catechin is necessary for Ag⁺ reduction, self-oxidisation of catechin also occurs at high pHs and/or high temperatures. This is likely the reason for the larger particle size for microwave assisted AgNPs prepared from catechin at pH 9. The size of AgNPs prepared with unmodified catechin was therefore minimised by using microwave assistance at pH 8.

Table 1: Surface plasmon resonance (dipolar) wavelength and absorbance, DLS particle size and PDI for prepared AgNPs

Reducing agent	pH	Borax (mM)	Reaction	SPR Peak (nm)	SPR Peak (abs)	Intensity mean	Number mean	Volume mean	PDI
Catechin	6	0	RT	n/p	n/p	n/m	n/m	n/m	n/m
Catechin	7	0	RT	n/p	n/p	407 ± 11	380 ± 14	457 ± 14	0.47 ± 0.02
Catechin	8	0	RT	n/p	n/p	232 ± 27	149.8 ± 4.9	274 ± 20	0.16 ± 0.01
Catechin	9	0	RT	436	1.17	171.7 ± 2.0	87.9 ± 6.0	194.6 ± 4.8	0.16±0.02
Catechin	6	0	Micro	n/p	n/p	n/m	n/m	n/m	n/m
Catechin	7	0	Micro	448	0.66	168.9 ± 2.4	107.6 ± 1.8	190.5 ± 4.6	0.21 ± 0.01
Catechin	8	0	Micro	430	0.93	153 ± 11	53 ± 26	128 ± 24	0.20 ± 0.01
Catechin	9	0	Micro	432	1.82	146.6 ± 0.6	108.0 ± 2.4	153.2 ± 1.0	0.08 ± 0.01
Catechin	7.8	0.5	RT	n/p	n/p	288 ± 14	240.1 ± 3.5	363 ± 35	0.15 ± 0.02
Catechin	8.1	1	RT	436	0.73	246 ± 18	205.1 ± 6.1	305 ± 41	0.17 ± 0.03
Catechin	8.4	2	RT	434	0.94	181.7 ± 3.0	152.8 ± 2.2	204.0 ± 4.3	0.07 ± 0.01
Catechin	8.6	3	RT	434	0.88	166.4 ± 1.8	131.7 ± 2.2	183.7 ± 0.4	0.08 ± 0.01
Catechin	7.8	0.5	Micro	431	1.10	175.5 ± 0.3	98.2 ± 0.5	203.7 ± 1.8	0.16 ± 0.01
Catechin	8.1	1	Micro	429	1.69	133.9 ± 3.4	62.7 ± 3.8	109.4 ± 4.2	0.19 ± 0.01
Catechin	8.4	2	Micro	406	2.31	118.7 ± 5.6	24.0 ± 5.5	44 ± 11	0.27 ± 0.01
Catechin	8.6	3	Micro	406	2.33	137.1 ± 1.1	21.1 ± 1.4	56 ± 11	0.22 ± 0.01
Polycat	6	0	RT	418	0.49	70.9 ± 0.9	35.9 ± 1.6	45.8 ± 1.2	0.17 ± 0.01
Polycat	7	0	RT	417	1.24	30.6 ± 1.5	16.6 ± 0.5	20.7 ± 0.4	0.15 ± 0.03
Polycat	8	0	RT	410	1.76	23.7 ± 0.4	15.4 ± 0.2	18.3 ± 0.2	0.09 ± 0.02
Polycat	9	0	RT	411	1.77	226 ± 58	11.3 ± 0.4	56 ± 20	0.36 ± 0.11
Polycat	6	0	Micro	410	1.54	30.8 ± 2.8	18.2 ± 0.2	22.1 ± 0.5	0.13 ± 0.03
Polycat	7	0	Micro	410	1.73	26.2 ± 0.2	17.6 ± 0.5	20.7 ± 0.4	0.08 ± 0.01
Polycat	8	0	Micro	410	1.91	29.5 ± 0.3	18.3 ± 0.3	22.1 ± 0.2	0.11 ± 0.01
Polycat	9	0	Micro	410	2.09	75 ± 34	15.6 ± 0.4	52 ± 26	0.17 ± 0.01

Notes: RT = room temperature; Micro = microwave; n/p = no peak observed; n/m = not measured

Cat-borax as reducing and capping agent

The gelation of polyvinyl alcohol or guar gum with borax to produce slime is a popular classroom experiment.⁹⁷ The tetrafunctional borate ion is able to hydrogen bond with four hydroxyl groups to form a 3D cross-linked network. As catechin contains five hydroxyl groups, we hypothesised that borax could be used as a cross-linker and thereby improve catechin's stabilising capacity via steric effects. **Scheme 1** shows one example of how this crosslinking could occur. DOSY NMR is commonly used to identify compounds in mixtures by separating the NMR signal based on differing diffusion coefficients with slower diffusion coefficients typically corresponding to higher hydrodynamic radius molecules. **Figure 2** shows an overlay of DOSY NMR spectra of catechin, cat-borax and polycat and indicates that cat-borax has a slower diffusion coefficient than catechin (-9.67 vs. -9.62 $\log \text{ m}^2/\text{s}$), thereby demonstrating that crosslinking has occurred. This is further supported by the shifts seen in the proton peaks (see ESI, **Figure S1**) for both B-ring (6.85 and 6.77 to 6.64 and 6.60 ppm, respectively) and C-ring protons (2.74 and 2.48 to 2.86 and 2.44 ppm, respectively). Note that the A-ring proton peaks are not visible due to proton-deuterium exchange, which is accelerated in ionic solutions.⁹⁸

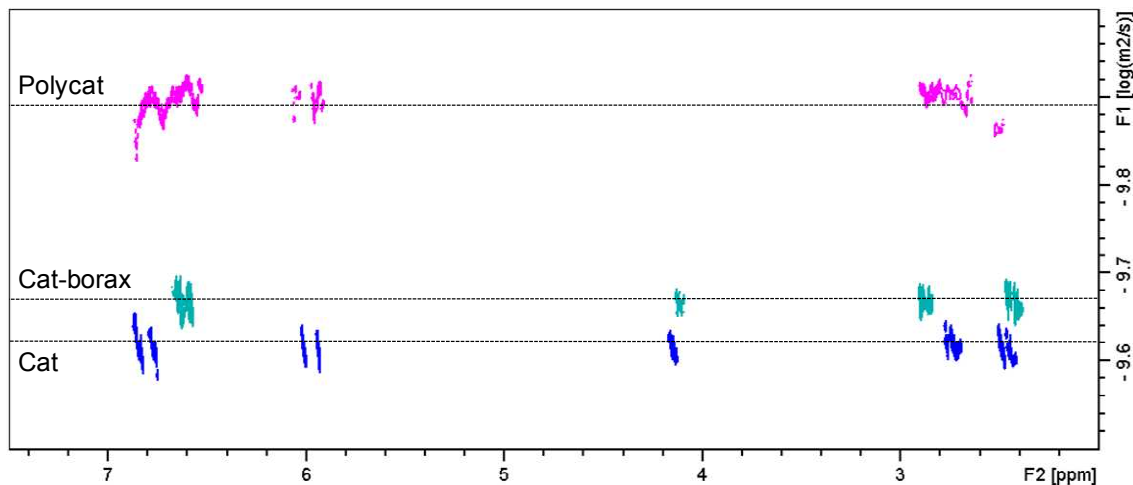


Figure 2: Overlay of DOSY NMR spectra of catechin (cat), cat-borax and polycat in 15% DMSO-d₆ / 85% D₂O.

Microwave assistance was found to produce smaller AgNPs prepared with cat-borax at all borax concentrations (**Figure 1c and d**). The concentration of borax required to improve catechin's stabilising capacity was optimised at 2 mM and further increases in concentration had a negligible effect on the SPR peak. (The ratio of catechin to borax used for DOSY NMR was the same as in the 2 mM cat-borax sample.) In contrast to AgNPs prepared with catechin, the SPR peaks for AgNPs prepared with cat-borax were readily distinguishable from oxidised catechin absorbance, suggesting smaller nanoparticles had been prepared. Indeed, optimised microwave-assisted cat-borax AgNPs were substantially smaller than those prepared from catechin alone (DLS number average size: 24 vs. 53 nm), demonstrating the improved stabilising effect of the cat-borax. Interestingly, for these cat-borax AgNPs, the DLS intensity average size is considerably higher than the number average size (118.7 vs. 24.0 nm), suggesting the presence of a small amount of larger particles in solution, however, no turbidity was noted in the UV-Vis spectrum. (See ESI, **Figure S2b** for DLS particle size distributions.)

Polycat as reducing and capping agent

We have previously shown that catechin can be polymerised in the presence of acid⁷⁶ (see **Scheme 1** for structure) and molecular weight and water solubility can be tuned by adjusting the reaction conditions. Polycat chosen for this study had a molecular weight (M_n) of 3600 g/mol (dispersity 1.4) and substantially greater water solubility than catechin (ca. 40 vs. 2.26 mg/mL). As mentioned above, greater water solubility improves the stabilising capacity of capping agents. Furthermore, as can be seen from **Figure 2**, polycat has a much slower diffusion coefficient ($-9.89 \log \text{ m}^2/\text{s}$) than either catechin or cat-borax, suggesting a considerably larger hydrodynamic radius and therefore better steric stabilisation. Finally, although measurements showed polycat had the same reducing capacity as catechin at each pH, nucleation appeared

to occur more rapidly when the polymer was used, possibly from the polymer structure providing more nucleation sites.

The increase in nucleation rate seen with polycat meant that small AgNPs were prepared at room temperature for $\text{pH} \geq 8$ (**Figure 1e**) so microwave assistance was not required to optimise size. Indeed, the SPR peak is readily distinguishable from oxidised polycat absorbance at all pHs, demonstrating that considerably smaller AgNPs were prepared with polycat than with catechin, even at low pHs. In line with the trend seen when catechin was used as reducing and capping agent, SPR wavelength generally decreased as pH increased (**Figure 1e** and **f**), suggesting smaller particle size. However, there is also evidence of increased polycat oxidation in the UV-Vis spectra at pH 9 and, although the DLS number average particle size (**Table 1**) was smaller for AgNPs prepared at pH 9 compared with pH 8, the volume average and intensity average particle size were considerably higher, suggesting that some agglomeration or aggregation occurred at the higher pH. This is consistent with the solubility of polycat decreasing slightly from increased quinone content. Optimal reaction conditions with polycat were therefore pH 8 and room temperature.

Interestingly, although AgNPs prepared with polycat at optimal conditions (pH 8 & room temperature) had a smaller size than those prepared with cat-borax, the SPR was at a slightly higher wavelength for those prepared with polycat (410 vs. 406 nm). This is likely owing to a red-shift in wavelength resulting from the association of the AgNPs with the polycat.

The enhanced stability offered by polycat was also apparent in the long-term stability of AgNP solutions prepared from polycat at pH 8, which were stable for at least six months. In contrast, particles began to precipitate after two days for AgNPs prepared from catechin and after one to two weeks for AgNPs prepared from cat-borax. However, AgNPs prepared by both methods could be easily redispersed,

suggesting agglomeration rather than aggregation. Finally, the stability of AgNPs prepared using polycat was apparent during centrifugation. Separating AgNPs from solution by centrifuging is a common method of purifying AgNPs prepared by both traditional⁹⁹ and green chemistry processes,^{42, 62, 63, 95, 100, 101} however, AgNPs prepared from polycat were too stable to be separated by this technique.

Characterisation of AgNPs

To further compare the effectiveness of catechin, cat-borax and polycat as reducing and capping agents for the preparation of AgNPs, the following three formulations were chosen for additional characterisation and antimicrobial testing: AgNPs prepared with catechin at pH 8 in microwave (Cat@AgNPs); AgNPs prepared with catechin and 2mM borax in microwave (Cat-borax@AgNPs); AgNPs prepared with polycat at pH 8 at room temperature (Polycat@AgNPs). Firstly, conversion of Ag^+ to AgNPs was determined by using ICP-MS to measure the silver content of the filtrate after centrifugal ultrafiltration of the AgNP solutions, and this showed that conversion of Ag^+ to AgNPs was greater than 99.99% for all three formulations. As conversion of Ag^+ was essentially complete and all reagents were benign, no purification was required.

XRD analysis of cat@AgNPs, cat-borax@AgNPs and polycat@AgNPs (**Figure 3**) identified 2θ peaks at 38.07, 44.26, 64.47 and 75.51°, which correspond to the (111), (200), (220) and (311) planes, respectively of FCC crystalline silver (ICDD card 00-001-1164). An additional small peak is visible on the cat@AgNPs spectrum at 32.27°, which suggests a small amount of surface oxidation may have occurred on these particles.¹⁰² The broader peaks seen for cat-borax@AgNPs and, in particular, polycat@AgNPs are indicative of their smaller particle sizes. Crystallite sizes as calculated by the Debye-Scherrer equation were 29.0, 18.7 and 9.3 nm for cat@AgNPs, cat-borax@AgNPs and polycat@AgNPs, respectively.

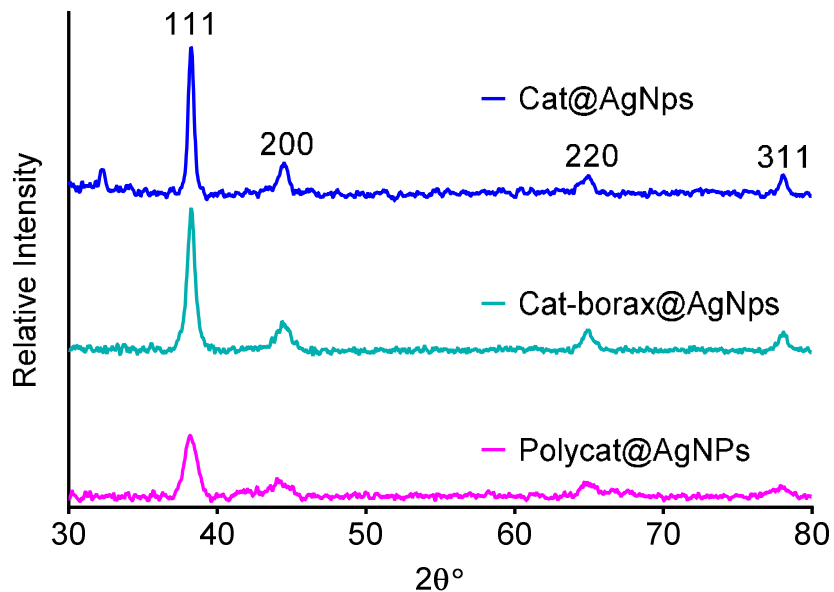


Figure 3: XRD spectra of cat@AgNPs, cat-borax@AgNPs and polycat@AgNPs

The size and morphology of the AgNPs were investigated through TEM imaging. Cat@AgNPs ranged in size from 10.2 to 107.4 nm with an average particle size of 42.3 nm. Particles were either spherical or irregular in shape (see **Figure 4a**) and some were present as agglomerates (see ESI, **Figure S3**), which ranged in size from 50 to 170 nm. Cat-borax@AgNPs were either spheres or ovoids (see **Figure 4b**) with a size distribution ranging from 9.3 to 29.9 nm and an average particle size of 18.4 nm. No larger agglomerates were found, which is consistent with the lack of turbidity seen in the UV-Vis spectrum. Polycat@AgNPs were considerably smaller (4.7 to 13.9 nm with an average size of 8.5 nm) and spherical in shape. The TEM image (**Figure 4c**) shows a clear polymeric layer around all AgNPs, demonstrating the nanoparticles are being stabilised by polycat.

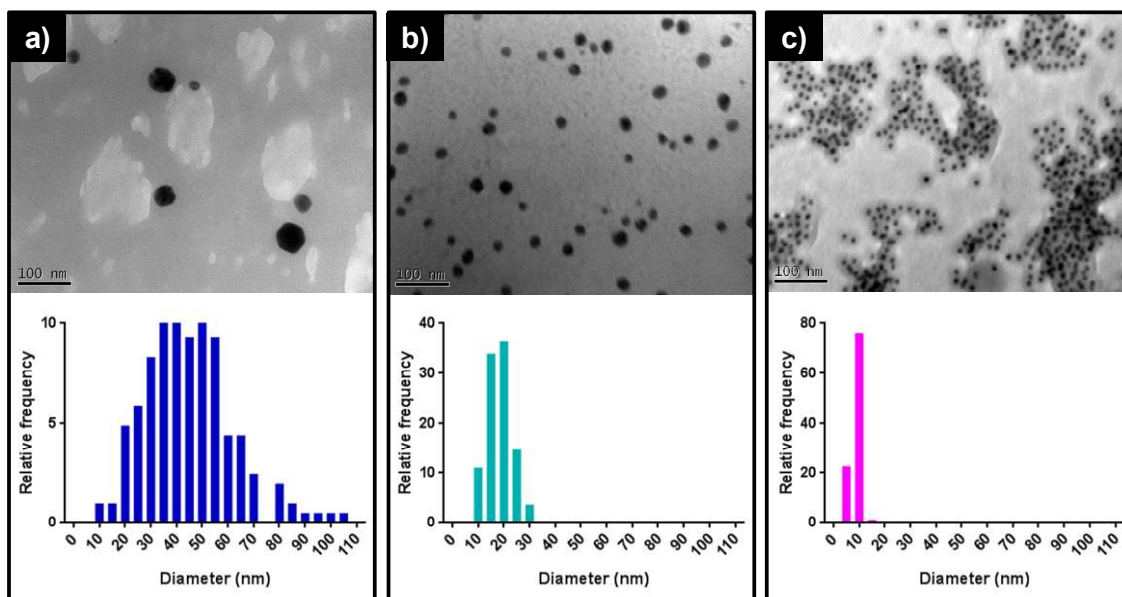


Figure 4: TEM images and frequency histograms for cat@AgNPs (a), cat-borax@AgNPs (b) and polycat@AgNPs (c). Histograms were determined from a minimum of 200 particles. All scale bars are 100 nm. No staining was used.

For cat-borax@AgNPs and polycat@AgNPs, particle size determined by TEM was consistent with crystallite size calculated from XRD, which suggests that these nanoparticles comprise primarily single crystals. In contrast, for cat@AgNPs, TEM particle size is larger than XRD crystal size, which is consistent with some cat@AgNPs being agglomerates (ESI, **Figure S3**). Number average size as determined by DLS was slightly higher for all nanoparticles compared with sizes observed by TEM (53 vs. 42.3 nm, 24.0 vs. 18.4 nm and 15.4 vs. 8.5 nm for cat@AgNPs, cat-borax@AgNPs and polycat@AgNPs, respectively). Other researchers have also found that DLS size measurements for AgNPs are higher than those determined by TEM^{30, 85, 93} and this can be attributed to the presence of the stabilising agent (cat-borax or polycat) increasing the hydrodynamic radius in solution and, in the case of cat@AgNPs and, to a lesser extent cat-borax@AgNPs, the presence of some agglomerates. (See ESI, **Figure S2** for DLS particle size distributions.) It should be noted that all three AgNPs have zeta potentials below -30 mV (-31.1±0.8 mV, -37.2±1.8 and -32.5±2.0 mV, for cat@AgNPs, cat-borax@AgNPs and polycat@AgNPs,

respectively) and thereby possess electrostatic stabilisation but only polycat@AgNPs have sufficient additional steric stabilisation to prevent agglomeration.

Evaluation of free radical scavenging activity

A number of the therapeutic benefits of catechin stem from its free radical scavenging activity⁷¹ and AgNPs are also known to scavenge free radicals⁹⁹ therefore it was important to assess whether this activity was maintained in cat@AgNPs, cat-borax@AgNPs and polycat@AgNPs. DPPH• is a stable free radical that is widely used to evaluate the free radical scavenging activity of antioxidants.¹⁰³ Consistent with our previous studies,⁷⁶ there is a modest (9.5 percentage points) but significant ($p = 0.0008$) improvement in the DPPH• inhibition of polycat over catechin (see **Figure 5**), however, there is no significant difference in DPPH• inhibition between catechin and cat@AgNPs or polycat and polycat@AgNPs. In contrast there is a significant ($p < 0.0001$) reduction (17.8 percentage points) in DPPH• inhibition for cat-borax@AgNPs compared with catechin. This is likely a result of some hydroxyl groups on catechin being unavailable for participation in reactions with free radicals owing to their bonding with borate groups (see **Scheme 1**).

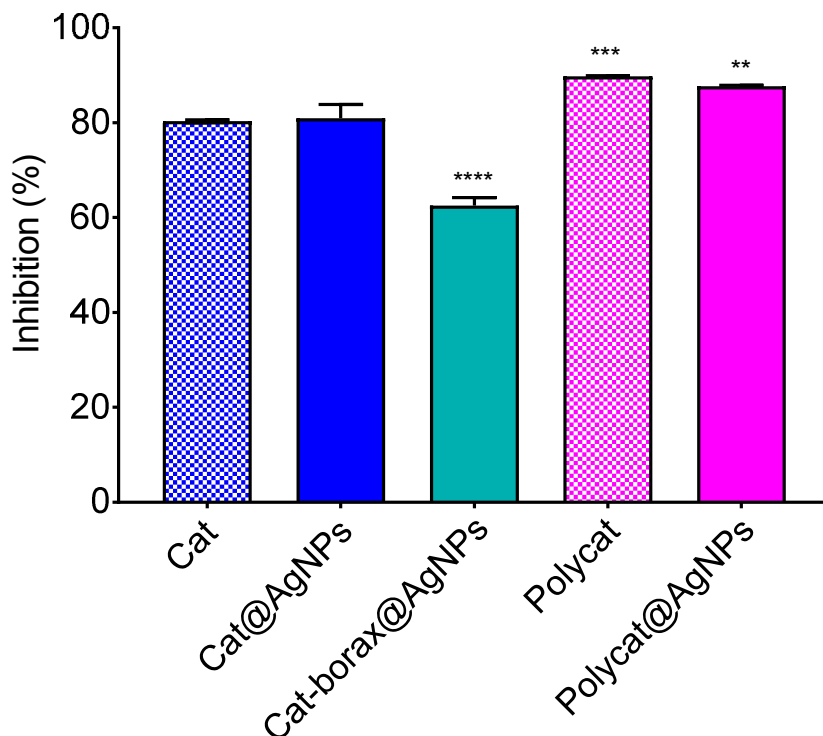


Figure 5: DPPH• scavenging of catechin (cat), cat@AgNPs, cat-borax@AgNPs, polycat and polycat@AgNPs. ** $p < 0.01$, *** $p < 0.001$, **** $p < 0.0001$ compared with cat.

Evaluation of antimicrobial activity (MIC)

Prior to evaluating the antimicrobial activity of cat@AgNPs, cat-borax@AgNPs, and polycat@AgNPs, the antimicrobial activity (MIC) of catechin and polycat was determined. Catechin and other flavonoids have long been known to possess antimicrobial activity albeit modest compared with available antibiotics.⁷²⁻⁷⁴ In line with the findings of other researchers,^{72, 104-106} catechin was found to be more efficacious against gram positive bacteria than gram negative bacteria (see **Table 2**), exhibiting an MIC of 2500-5,000 $\mu\text{g/mL}$ against *S. aureus* (gram positive) compared with 10,000 $\mu\text{g/mL}$ against the three gram negative bacteria tested (*E. coli*, *P. aeruginosa* and *A. baumannii*). One of the key modes of action of catechin is believed to be membrane disruption and the lower efficacy against gram negative bacteria can, in part, be attributed to them containing less peptidoglycan, which binds catechin,^{105, 106} as well as some repulsion from the negatively charged lipid bilayer.^{72,}

Table 2: Antimicrobial activity (MIC) of catechin and polycat.

Bacteria	MIC ($\mu\text{g/mL}$)	
	Catechin	Polycat
<i>E. coli</i>	10,000	1,000
<i>P. aeruginosa</i>	10,000	1,000
<i>A. baumannii</i>	10,000	500
<i>S. aureus</i>	2500-5,000	125

A substantial improvement in antimicrobial efficacy was seen for polycat compared with catechin with MIC values decreasing 10-fold for *E. coli* and *P. aeruginosa*; 20-fold for *A. baumannii*; and 20 to 40-fold for *S. aureus* (**Table 2**). In contrast, when the polyphenols rutin¹⁰⁷ or tannic acid¹⁰⁸ are polymerised, antimicrobial efficacy decreases. The improvement in antimicrobial efficacy for polycat is therefore unlikely to be simply a result of its polymeric nature and is possibly related to its improved water solubility (see above) as an increase in hydrophilicity is believed to preserve antimicrobial efficacy through reduction in unwanted protein complexation.^{78, 109}

The antimicrobial inhibitory activity of cat@AgNPs, cat-borax@AgNPs and polycat@AgNPs is presented in **Table 3** and all three AgNP formulations show better activity against gram negative bacteria (*E. coli*, *P. aeruginosa* and *A. baumannii*) than gram positive bacteria (*S. aureus*), which is in line with the findings of other researchers,^{22, 61, 110-112} Indeed, for cat@AgNPs and cat-borax@AgNPs, no MICs were reached for *S. aureus* at the concentrations tested. The difference in activity of AgNPs between gram negative and gram positive bacteria can be attributed to the difference in structure of their cell walls. The greater thickness, rigidity and cross-linking in gram positive bacteria provides fewer anchoring sites for silver nanoparticles as well as making the cell wall more difficult to penetrate.¹¹¹

Table 3: Antimicrobial activity (MIC) of cat@AgNPs, cat-borax@AgNPs and polycat@AgNPs.

Bacteria	MIC ($\mu\text{g/mL}$) silver (catechin)			
	Cat@AgNPs	Cat-borax@AgNPs	Polycat@AgNPs	Citrate@AgNPs

<i>E. coli</i>	20 (108)	20 (108)	2.5 (13)	20
<i>P. aeruginosa</i>	10 (54)	5 (27)	1.25 (7)	5
<i>A. baumannii</i>	20 (108)	10 (54)	1.25 (7)	20
<i>S. aureus</i>	>20 (>108)	>20 (>108)	5 (27) – 10 (54)	20

Note: Data is presented based on silver concentrations. The concentration of catechin (or polycat) also present is shown in brackets. Citrate@AgNPs are 10 nm commercial sodium citrate capped AgNPs.

For all bacteria tested, polycat@AgNPs exhibited the lowest MICs and, importantly, for *P. aeruginosa* and *A. baumannii*, which have been identified by the World Health Organization as “priority pathogens,”¹¹³ the MIC was only 1.25 µg/mL. In general, cat-borax@AgNPs had lower MICs than cat@AgNPs. For *E. coli*, although MICs were 20 µg/mL for both, at a concentration of 10 µg/mL cat-borax@AgNPs had an inhibition of 72 ± 10% whereas for cat@AgNPs it was only 44 ± 7%. The improvements in antimicrobial efficacy can partly be explained by the decrease in particle size from cat@AgNPs (42.3 nm) to cat-borax@AgNPs (18.4 nm) to polycat@AgNPs (8.5 nm) as the increased surface area and greater penetrating ability from smaller particle size has been identified by a number of researchers as leading to greater efficacy.^{61, 112, 114}

We also hypothesised that the use of polycat as the capping agent played a role in the improved antimicrobial efficacy of polycat@AgNPs and to confirm this MICs were determined for similarly sized (10 nm) commercially available sodium citrate capped AgNPs (citrate@AgNPs), like polycat@AgNPs, have a zeta potential below -30 mV.^{112, 115} These results are also presented in **Table 3** and confirm that polycat@AgNPs have superior antimicrobial efficacy to citrate@AgNPs, demonstrating between 2 and 16-fold improvement in MICs. A number of researchers have explored the effect of capping agents on antimicrobial efficacy and have demonstrated that antimicrobial efficacy varies with choice of capping agent.¹¹⁶⁻¹¹⁸ For instance, Kvittek *et al.*¹¹⁸ showed that antimicrobial efficacy of AgNPs was improved when capping agents were added and demonstrated that polyvinylpyrrolidone (PVP) and sodium dodecyl sulfate (SDS) provided greater

improvement than polyoxyethylenesorbitane monooleate (Tween 80). It is worth noting, however, that the weight ratio of polymer and/or surfactant to Ag used in this study was substantially higher than the ratio of polycat to Ag (93:1 vs. 5:1), suggesting that polycat may provide superior antimicrobial enhancement.

Evaluation of antibiofilm activity

Bacteria embedded in biofilm, a self-produced polymer matrix comprising polysaccharide, protein and DNA, are typically more difficult to eradicate than planktonic bacteria.^{5,6} The bactericidal efficacy of the three AgNP formulations was assessed after 60 min treatment at a Ag concentration of 5 µg/mL against biofilms prepared from the opportunistic bacteria *P. aeruginosa* PAO1 (see **Figure 6**).

Treatment with cat@AgNPs and cat-borax@AgNPs delivered modest reductions in cell viability for both planktonic and biofilm bacteria and, in contrast to inhibitory effects, no significant difference was observed in the efficacy of the two AgNP formulations. Citrate@AgNPs had no significant effect on either planktonic or biofilm bacteria. On the other hand, treatment with polycat@AgNPs yielded excellent bactericidal efficacy, displaying 99.9% reduction in both planktonic and biofilm bacteria.

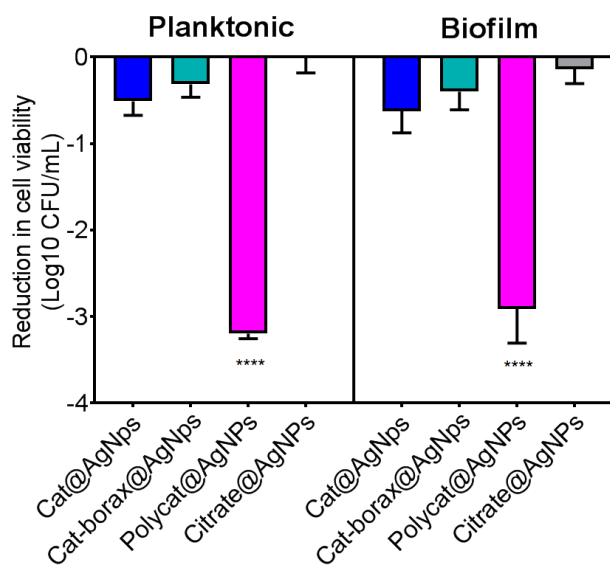


Figure 6: Reduction in cell viability of *P. aeruginosa* planktonic and biofilm bacteria following 60 min treatment with 5 µg/mL of cat@AgNPs, cat-borax@AgNPs, polycat@AgNPs and citrate@AgNPs. ****p<0.0001 compared with cat@AgNPs.

Successful eradication of biofilm involves dispersing as well as killing biofilm bacteria and often there is no correlation between the two with many treatments only achieving one or the other.²² Crystal violet (CV) staining is typically used to quantify biofilm dispersal,^{78, 119, 120} however, it was found unsuitable for evaluating our AgNPs owing to absorption of CV by catechin and polycat. Biofilms were therefore quantified by determining the biofilm volume via digital staining from images captured from at least eight different regions with a 3D tomographic microscope. Representative images of untreated and treated biofilms are presented in **Figure 7**. The untreated biofilm layer was approximately 5 µm thick and no reduction in biofilm volume was seen for biofilms treated with cat@AgNPs, cat-borax@AgNPs or citrate@AgNPs but a substantial $99.1 \pm 0.7\%$ reduction was measured for biofilms treated with polycat@AgNPs. Therefore, 5 µg/mL of polycat@AgNPs is able to both kill and disperse biofilms after 60 mins treatment. To

the best of our knowledge this is the lowest reported concentration of AgNPs to successfully eradicate biofilms.

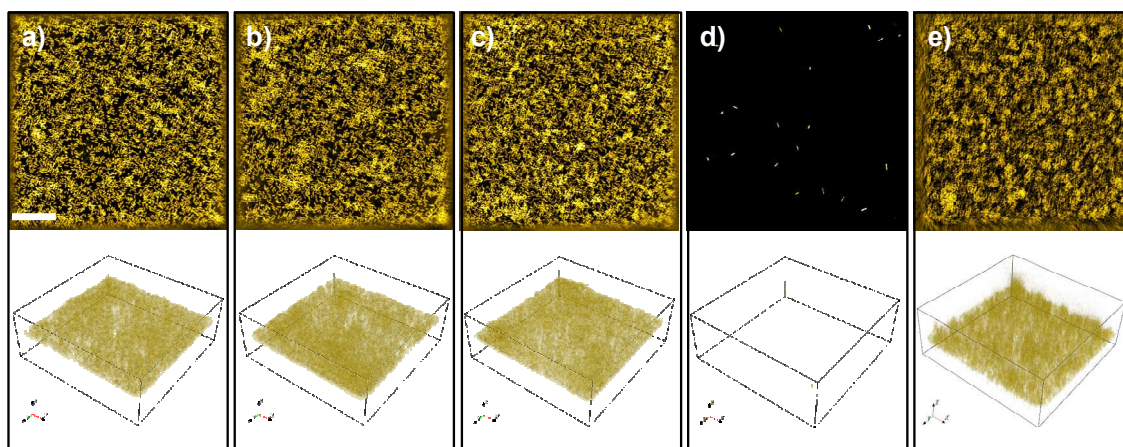


Figure 7: Representative 2D and 3D tomographic microscopy images of untreated biofilm (a) and biofilm treated with cat@AgNPs (b), cat-borax@AgNPs (c), polycat@AgNPs (d) or citrate@AgNPs (e). Scale bar is 20 μm .

As with inhibitory effects, the ability of AgNPs to disperse nanoparticles increases with decreases in particle size. Loo *et al.* reported biofilm removal efficiency of 90%, 69% and 52% for *P. aeruginosa* biofilms grown in M9 medium treated with 600 $\mu\text{g/mL}$ of AgNPs with 8, 20 and 35 nm diameters, respectively.¹² Although differences in methodology mean results are not directly comparable, the substantially higher concentration of 8 nm AgNPs required to reduce biofilm by 90% (600 $\mu\text{g/mL}$) compared with the concentration of 8.5 nm polycat@AgNPs for a 99.1% reduction (5 $\mu\text{g/mL}$) strongly suggests that polycat substantially enhances biofilm dispersal. This is further supported by our data showing no biofilm is eradicated when treated with 5 $\mu\text{g/mL}$ of 10 nm citrate@AgNPs. Catechin is believed to exert *P. aeruginosa* antibiofilm activity through the attenuation of quorum sensing¹²¹ and, therefore, it is likely that polycat exhibits similar activity. However, no significant reduction in biomass was observed when biofilms were treated with polycat at the equivalent concentration to that in polycat@AgNPs (i.e., 27 $\mu\text{g/mL}$) so the excellent antibiofilm results achieved with polycat@AgNPs are likely a synergistic effect.

To help elucidate why polycat enhances the antimicrobial efficacy of AgNPs, further analysis was undertaken with the similarly sized polycat@AgNPs and citrate@AgNPs. Firstly, tomographic microscopy and SEM images were captured of planktonic *P. aeruginosa* bacteria following treatment with 5 $\mu\text{g}/\text{mL}$ of polycat@AgNPs or citrate@AgNPs for 60 mins. The tomographic images (**Figure 8**, top) depict unadulterated bacterial suspensions and have been digitally stained. We were surprised to note that treatment with polycat@AgNPs (**Figure 8b**) resulted in approximately 70% reduction (measured by digital stain volume) in bacterial cell numbers. No reduction in cell numbers was observed following treatment with citrate@AgNPs (**Figure 8c**) and treatment of *P. aeruginosa* with AgNPs for 24 h at concentrations as high as 500 $\mu\text{g}/\text{mL}$ has previously been shown to have no effect on cell numbers although bacteria were largely non-culturable.¹²² Examination of SEM images (**Figure 8**, bottom) confirms bacteria cell destruction following treatment with polycat@AgNPs. Detritus from destroyed bacteria cells (see pink arrows) are clearly visible on the SEM image of cells treated with polycat@AgNPs (**Figure 8b**) but were not found on any images of cells treated with citrate@AgNPs (**Figure 8c**) or untreated cells (**Figure 8a**). Some cells treated with citrate@AgNPs did, however, show evidence of membrane damage (blue arrows) as did remaining cells treated with polycat@AgNPs.

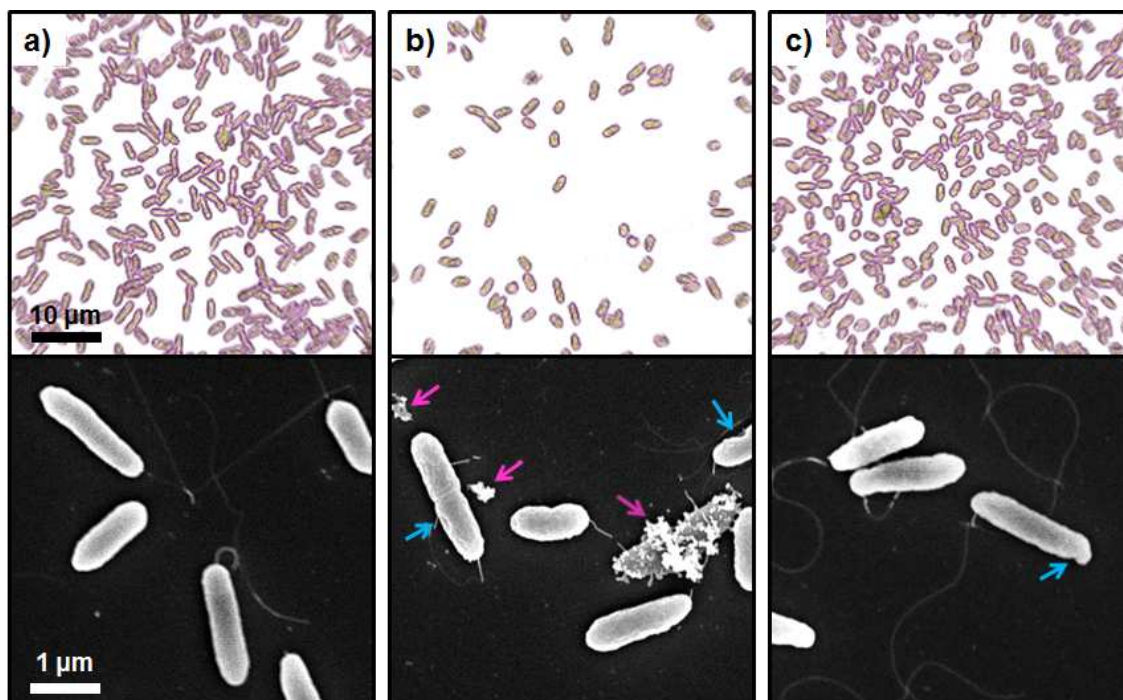


Figure 8: Representative tomographic microscopy (top) and SEM (bottom) images of untreated *P. aeruginosa* planktonic bacteria (a) and after 60 min treatment with 5 µg/mL polycat@AgNPs (b) or citrate@AgNPs (c).

One mechanism by which AgNPs exert antimicrobial activity is through the release of silver ions.²¹⁻²³ To determine if Ag⁺ release was involved in the enhanced antimicrobial activity of polycat@AgNPs, we compared the Ag⁺ release behaviour of 5 µg/mL of polycat@AgNPs and citrate@AgNPs after 60 min incubation in M9 complete media under the same conditions as were used for the bacteria killing assessment. Interestingly, citrate@AgNPs showed release of 9 ± 6 µg/L Ag⁺ whereas the measured concentration of Ag⁺ released from polycat@AgNPs by ICP-MS was below the limit of reporting (2 µg/L) of the instrument. Release of Ag⁺ is therefore not a factor in the improved antibacterial efficacy of polycat@AgNPs. The low release of Ag⁺ is likely owing to the reduction of Ag⁺ back to Ag⁰ by polycat.

AgNPs can also exhibit antimicrobial efficacy through direct contact with bacteria cells and this mode of action is particularly apparent in AgNPs sized 10 nm or below.²⁰ **Figure 9** shows the silver uptake of *P. aeruginosa* after 60 min treatment with

5 $\mu\text{g/mL}$ polycat@AgNPs or citrate@AgNPs and clearly demonstrates that uptake of polycat@AgNPs was significantly higher than citrate@AgNPs. Indeed, uptake of polycat@AgNPs was over 20 times higher than citrate@AgNPs and therefore the use of polycat as a capping agent greatly increased contact between AgNPs and bacteria cells thereby improving antibacterial efficacy. Catechin is known to bind with peptidoglycan^{105, 106} and therefore it is likely that polycat facilitates attachment of AgNPs to bacteria via this route. Membrane damage from the attached AgNPs is also likely to increase polycat penetration of the bacteria cells thereby potentiating polycat's antibacterial effect.

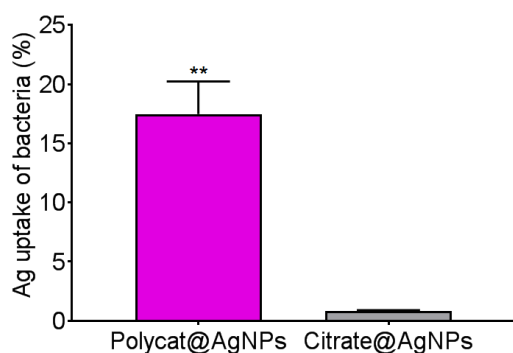


Figure 9: Silver uptake of *P. aeruginosa* after 60 min treatment with 5 $\mu\text{g/mL}$ polycat@AgNPs or citrate@AgNPs. ** $p < 0.01$ compared with citrate@AgNPs.

Conclusion

AgNPs were prepared using catechin, cat-borax or polycat as both reducing and capping agents. Cat-borax produced smaller AgNPs than catechin but the smallest particles were prepared with polycat. Polycat@AgNPs showed superior antimicrobial activity to cat@AgNPs and cat-borax@AgNPs against both gram negative and gram positive bacteria and also demonstrated substantially enhanced antibiofilm activity. Polycat@AgNPs also showed improved antimicrobial activity compared with similarly sized citrate@AgNPs. An Ag concentration of only 5 $\mu\text{g/mL}$, was sufficient for a 99.9% reduction in biofilm cell viability and a 99.1% reduction in biofilm biomass with polycat@AgNPs. The use of polycat as a capping

agent increased contact between AgNPs and bacteria cells thereby improving antibacterial efficacy. The technique used to prepare polycat can also be adapted to prepare polymers from other polyphenols, including quercetin⁷⁶ and green tea extract (data not shown) so could potentially be used to enhance the antimicrobial efficacy of AgNPs prepared from various polyphenol rich plant extracts.

Acknowledgements

The authors would like to acknowledge the NMR Facility within the Mark Wainwright Analytical Centre at the University of New South Wales for NMR support. The authors thank Dr Nicholas Ariotti and Dr Yin Yao for technical assistance and use of facilities at the Electron Microscope Unit at UNSW. SO acknowledges support through an Australian Government Research Training Program Scholarship. CB acknowledges Australian Research Council (ARC) for his Future Fellowship (FT12010090).

References

1. G. D. Wright, *ACS Infectious Diseases*, 2015, 1, 80-84.
2. J. H. Rex, B. I. Eisenstein, J. Alder, M. Goldberger, R. Meyer, A. Dane, I. Friedland, C. Knirsch, W. R. Sanhai, J. Tomayko, C. Lancaster and J. Jackson, *The Lancet Infectious Diseases*, 13, 269-275.
3. G. D. Wright, *Trends Microbiol.*, 24, 862-871.
4. D. M. Brogan and E. Mossialos, *Globalization and Health*, 2016, 12, 8.
5. W. Costerton, R. Veeh, M. Shirtliff, M. Pasmore, C. Post and G. Ehrlich, *J. Clin. Invest.*, 2003, 112, 1466-1477.
6. N. Høiby, T. Bjarnsholt, M. Givskov, S. Molin and O. Ciofu, *Int. J. Antimicrob. Agents*, 35, 322-332.
7. M. Rai, A. Yadav and A. Gade, *Biotechnol. Adv.*, 2009, 27, 76-83.
8. M. K. Rai, S. D. Deshmukh, A. P. Ingle and A. K. Gade, *J. Appl. Microbiol.*, 2012, 112, 841-852.
9. G. Franci, A. Falanga, S. Galdiero, L. Palomba, M. Rai, G. Morelli and M. Galdiero, *Molecules*, 2015, 20, 8856.

10. C. Y. Loo, R. Rohanizadeh, P. Young, D. Traini, R. Cavaliere, C. Whitchurch and W. h. Lee, *Combination of Silver Nanoparticles and Curcumin Nanoparticles for Enhanced Anti-biofilm Activities*, 2015.
11. H.-J. Park, S. Park, J. Roh, S. Kim, K. Choi, J. Yi, Y. Kim and J. Yoon, *Journal of Industrial and Engineering Chemistry*, 2013, 19, 614-619.
12. C.-Y. Loo, P. M. Young, R. Cavaliere, C. B. Whitchurch, W.-H. Lee and R. Rohanizadeh, *Drug Dev. Ind. Pharm.*, 2014, 40, 719-729.
13. M. A. Radzig, V. A. Nadtochenko, O. A. Koksharova, J. Kiwi, V. A. Lipasova and I. A. Khmel, *Colloids Surf. B. Biointerfaces*, 2013, 102, 300-306.
14. S. Prabhu and E. K. Poulouse, *International Nano Letters*, 2012, 2, 32.
15. C. Marambio-Jones and E. M. V. Hoek, *J. Nanopart. Res.*, 2010, 12, 1531-1551.
16. B. Reidy, A. Haase, A. Luch, A. K. Dawson and I. Lynch, *Materials*, 2013, 6.
17. N. Durán, M. Durán, M. B. de Jesus, A. B. Seabra, W. J. Fávaro and G. Nakazato, *Nanomed. Nanotechnol. Biol. Med.*, 2016, 12, 789-799.
18. I. Sondi and B. Salopek-Sondi, *J. Colloid Interface Sci.*, 2004, 275, 177-182.
19. C.-N. Lok, C.-M. Ho, R. Chen, Q.-Y. He, W.-Y. Yu, H. Sun, P. K.-H. Tam, J.-F. Chiu and C.-M. Che, *J. Proteome Res.*, 2006, 5, 916-924.
20. M. Jose Ruben, E. Jose Luis, C. Alejandra, H. Katherine, B. K. Juan, R. Jose Tapia and Y. Miguel Jose, *Nanotechnology*, 2005, 16, 2346.
21. B. Le Ouay and F. Stellacci, *Nano Today*, 2015, 10, 339-354.
22. Q. L. Feng, J. Wu, G. Q. Chen, F. Z. Cui, T. N. Kim and J. O. Kim, *J. Biomed. Mater. Res.*, 2000, 52, 662-668.
23. G. A. Sotiriou and S. E. Pratsinis, *Environ. Sci. Technol.*, 2010, 44, 5649-5654.
24. V. F. Cardozo, A. G. Oliveira, E. K. Nishio, M. R. Perugini, C. G. Andrade, W. D. Silveira, N. Durán, G. Andrade, R. K. Kobayashi and G. Nakazato, *Ann. Clin. Microbiol. Antimicrob.*, 2013, 12, 12.
25. R. Perugini Biasi-Garbin, E. Saori Otaguiri, A. T. Morey, M. Fernandes da Silva, A. E. Belotto Morguette, C. Armando Contreras Lancheros, #xe9, sar, D. Kian, M. Perugini, #xe1, r. R. Eches, G. Nakazato, Dur, #xe1, N. n, C. V. Nakamura, L. M. Yamauchi and S. F. Yamada-Ogatta, *Evid. Based Complement. Alternat. Med.*, 2015, 2015, 8.
26. L. Ping, L. Juan, W. Changzhu, W. Qingsheng and L. Jian, *Nanotechnology*, 2005, 16, 1912.
27. G. Thirumurugan, J. V. L. N. Seshagiri Rao and M. D. Dhanaraju, *Sci. Rep.*, 2016, 6, 29982.
28. I. N. Ghosh, S. D. Patil, T. K. Sharma, S. K. Srivastava, R. Pathania and N. K. Navani, *International Journal of Nanomedicine*, 2013, 8, 4721-4731.
29. D. Hebbalalu, J. Lalley, M. N. Nadagouda and R. S. Varma, *ACS Sustainable Chemistry & Engineering*, 2013, 1, 703-712.
30. X.-F. Zhang, Z.-G. Liu, W. Shen and S. Gurunathan, *Int. J. Mol. Sci.*, 2016, 17, 1534.
31. V. K. Sharma, R. A. Yngard and Y. Lin, *Adv. Colloid Interface Sci.*, 2009, 145, 83-96.

32. S. Iravani, *Green Chem.*, 2011, 13, 2638-2650.
33. R. Mohammadinejad, S. Karimi, S. Iravani and R. S. Varma, *Green Chem.*, 2016, 18, 20-52.
34. K. S. Siddiqi, A. Husen and R. A. K. Rao, *Journal of Nanobiotechnology*, 2018, 16, 14.
35. P. Sathishkumar, F. L. Gu, Q. Zhan, T. Palvannan and A. R. Mohd Yusoff, *Mater. Lett.*, 2018, 210, 26-30.
36. G. Marslin, R. K. Selvakesavan, G. Franklin, B. Sarmento and A. C. P. Dias, *International Journal of Nanomedicine*, 2015, 10, 5955-5963.
37. M. N. Nadagouda and R. S. Varma, *Green Chem.*, 2008, 10, 859-862.
38. M. C. Moulton, L. K. Braydich-Stolle, M. N. Nadagouda, S. Kunzelman, S. M. Hussain and R. S. Varma, *Nanoscale*, 2010, 2, 763-770.
39. M. Nakhjavani, V. Nikkhah, M. M. Sarafraz, S. Shoja and M. Sarafraz, *Heat Mass Transfer.*, 2017, 53, 3201-3209.
40. Q. Sun, X. Cai, J. Li, M. Zheng, Z. Chen and C.-P. Yu, *Colloids Surf. Physicochem. Eng. Aspects*, 2014, 444, 226-231.
41. A. K. Mittal, J. Bhaumik, S. Kumar and U. C. Banerjee, *J. Colloid Interface Sci.*, 2014, 415, 39-47.
42. J. R. Nakkala, R. Mata, A. K. Gupta and S. R. Sadras, *Eur. J. Med. Chem.*, 2014, 85, 784-794.
43. V. Kumar, S. C. Yadav and S. K. Yadav, *J. Chem. Technol. Biotechnol.*, 2010, 85, 1301-1309.
44. M. Sathishkumar, K. Sneha, S. W. Won, C. W. Cho, S. Kim and Y. S. Yun, *Colloids Surf. B. Biointerfaces*, 2009, 73, 332-338.
45. A. R. Vilchis-Nestor, V. Sánchez-Mendieta, M. A. Camacho-López, R. M. Gómez-Espinosa, M. A. Camacho-López and J. A. Arenas-Alatorre, *Mater. Lett.*, 2008, 62, 3103-3105.
46. S. Iravani and B. Zolfaghari, *BioMed Research International*, 2013, 2013, 5.
47. K. Mohan Kumar, M. Sinha, B. K. Mandal, A. R. Ghosh, K. Siva Kumar and P. Sreedhara Reddy, *Spectrochimica Acta Part A: Molecular and Biomolecular Spectroscopy*, 2012, 91, 228-233.
48. K. Rajaram, D. C. Aiswarya and P. Sureshkumar, *Mater. Lett.*, 2015, 138, 251-254.
49. N. A. Begum, S. Mondal, S. Basu, R. A. Laskar and D. Mandal, *Colloids Surf. B. Biointerfaces*, 2009, 71, 113-118.
50. A. K. Jha, K. Prasad, K. Prasad and A. R. Kulkarni, *Colloids Surf. B. Biointerfaces*, 2009, 73, 219-223.
51. J. Huang, G. Zhan, B. Zheng, D. Sun, F. Lu, Y. Lin, H. Chen, Z. Zheng, Y. Zheng and Q. Li, *Ind. Eng. Chem. Res.*, 2011, 50, 9095-9106.
52. A. R. Im, L. Han, E. R. Kim, J. Kim, Y. S. Kim and Y. Park, *Phytother. Res.*, 2012, 26, 1249-1255.
53. C. Ramteke, T. Chakrabarti, B. K. Sarangi and R.-A. Pandey, *Journal of Chemistry*, 2013, 2013, 7.

54. M. R. Bindhu and M. Umadevi, *Spectrochimica Acta Part A: Molecular and Biomolecular Spectroscopy*, 2014, 128, 37-45.
55. E. C. Njagi, H. Huang, L. Stafford, H. Genuino, H. M. Galindo, J. B. Collins, G. E. Hoag and S. L. Suib, *Langmuir*, 2011, 27, 264-271.
56. N. Muniyappan and N. S. Nagarajan, *Process Biochem.*, 2014, 49, 1054-1061.
57. N. Jayaprakash, J. J. Vijaya, K. Kaviyarasu, K. Kombaiyah, L. J. Kennedy, R. J. Ramalingam, M. A. Munusamy and H. A. Al-Lohedan, *J. Photochem. Photobiol. B: Biol.*, 2017, 169, 178-185.
58. G. M. Nazeruddin, N. R. Prasad, S. R. Prasad, Y. I. Shaikh, S. R. Waghmare and P. Adhyapak, *Industrial Crops and Products*, 2014, 60, 212-216.
59. C. Krishnaraj, R. Ramachandran, K. Mohan and P. T. Kalaichelvan, *Spectrochimica Acta Part A: Molecular and Biomolecular Spectroscopy*, 2012, 93, 95-99.
60. B. S. Amedea, M. Nixson, L. Bruna de Araujo, T. P. Milena, B. Marcelo, R. Olga and D. Nelson, *Journal of Physics: Conference Series*, 2017, 838, 012031.
61. G. A. Martínez-Castañón, N. Niño-Martínez, F. Martínez-Gutierrez, J. R. Martínez-Mendoza and F. Ruiz, *J. Nanopart. Res.*, 2008, 10, 1343-1348.
62. A. K. Mittal, S. Kumar and U. C. Banerjee, *J. Colloid Interface Sci.*, 2014, 431, 194-199.
63. N. Zhang, J. Luo, R. Liu and X. Liu, *RSC Advances*, 2016, 6, 83720-83729.
64. Y. Hao, N. Zhang, J. Luo and X. Liu, *Nano*, 2018, 13, 1850003.
65. M. Rafique, I. Sadaf, M. S. Rafique and M. B. Tahir, *Artificial Cells, Nanomedicine, and Biotechnology*, 2017, 45, 1272-1291.
66. F. Di Renzo, *Catal. Today*, 1998, 41, 37-40.
67. N. T. K. Thanh, N. Maclean and S. Mahiddine, *Chem. Rev.*, 2014, 114, 7610-7630.
68. B. He, J. J. Tan, K. Y. Liew and H. Liu, *J. Mol. Catal. A: Chem.*, 2004, 221, 121-126.
69. J. Polte, *CrystEngComm*, 2015, 17, 6809-6830.
70. M. Cinelli, S. R. Coles, M. N. Nadagouda, J. Blaszczynski, R. Slowinski, R. S. Varma and K. Kirwan, *Green Chem.*, 2015, 17, 2825-2839.
71. S. Oliver, O. Vittorio, G. Cirillo and C. Boyer, *Polymer Chemistry*, 2016, 7, 1529-1544.
72. T. P. T. Cushnie and A. J. Lamb, *Int. J. Antimicrob. Agents*, 2005, 26, 343-356.
73. T. P. T. Cushnie and A. J. Lamb, *Int. J. Antimicrob. Agents*, 2011, 38, 99-107.
74. W. C. Reygaert, *Front. Microbiol.*, 2014, 5, 434.
75. C. Bellmann, *Chemical Engineering & Technology*, 2004, 27, 937-942.
76. S. Oliver, J. M. Hook and C. Boyer, *Polymer Chemistry*, 2017, 8, 2317-2326.
77. D. Qiao, C. Ke, B. Hu, J. Luo, H. Ye, Y. Sun, X. Yan and X. Zeng, *Carbohydr. Polym.*, 2009, 78, 199-204.
78. T.-K. Nguyen, S. J. Lam, K. K. K. Ho, N. Kumar, G. G. Qiao, S. Egan, C. Boyer and E. H. H. Wong, *ACS Infectious Diseases*, 2017, 3, 237-248.
79. A. Bax, *Journal of Magnetic Resonance (1969)*, 1985, 65, 142-145.

80. K. F. Morris and C. S. Johnson, *J. Am. Chem. Soc.*, 1992, 114, 3139-3141.
81. D. C. Skillman and C. R. Berry, *J. Opt. Soc. Am.*, 1973, 63, 707-713.
82. D. Paramelle, A. Sadovoy, S. Gorelik, P. Free, J. Hobley and D. G. Fernig, *Analyst*, 2014, 139, 4855-4861.
83. S. Bayram, O. K. Zahr and A. S. Blum, *RSC Advances*, 2015, 5, 6553-6559.
84. O. Tzhayik, P. Sawant, S. Efrima, E. Kovalev and J. T. Klug, *Langmuir*, 2002, 18, 3364-3369.
85. P. Quaresma, L. Soares, L. Contar, A. Miranda, I. Osorio, P. A. Carvalho, R. Franco and E. Pereira, *Green Chem.*, 2009, 11, 1889-1893.
86. N. G. Bastús, F. Merkoçi, J. Piella and V. Puntès, *Chem. Mater.*, 2014, 26, 2836-2846.
87. S. Oliver, D. S. Thomas, M. Kavallaris, O. Vittorio and C. Boyer, *Polymer Chemistry*, 2016, 7, 2542-2552.
88. S. Oliver, E. Yee, M. Kavallaris, O. Vittorio and C. Boyer, *Macromol. Biosci.*, DOI: 10.1002/mabi.201700239, 1700239-n/a.
89. S. Nishimura, D. Mott, A. Takagaki, S. Maenosono and K. Ebitani, *PCCP*, 2011, 13, 9335-9343.
90. B. Baruwati, V. Polshettiwar and R. S. Varma, *Green Chem.*, 2009, 11, 926-930.
91. J. M. Patete, X. Peng, C. Koenigsmann, Y. Xu, B. Karn and S. S. Wong, *Green Chem.*, 2011, 13, 482-519.
92. S. Francis, S. Joseph, E. P. Koshy and B. Mathew, *Artificial Cells, Nanomedicine, and Biotechnology*, 2017, DOI: 10.1080/21691401.2017.1345921, 1-10.
93. G. A. Kahrilas, L. M. Wally, S. J. Fredrick, M. Hiskey, A. L. Prieto and J. E. Owens, *ACS Sustainable Chemistry & Engineering*, 2014, 2, 367-376.
94. M. N. Nadagouda, T. F. Speth and R. S. Varma, *Acc. Chem. Res.*, 2011, 44, 469-478.
95. B. Hu, S.-B. Wang, K. Wang, M. Zhang and S.-H. Yu, *The Journal of Physical Chemistry C*, 2008, 112, 11169-11174.
96. I. Fatimah, *Journal of Advanced Research*, 2016, 7, 961-969.
97. E. Z. Casassa, A. M. Sarquis and C. H. Van Dyke, *J. Chem. Educ.*, 1986, 63, 57.
98. S. Oliver, A. Jofri, D. S. Thomas, O. Vittorio, M. Kavallaris and C. Boyer, *Carbohydr. Polym.*, 2017, 169, 480-494.
99. M. Jokar, R. A. Rahman, N. A. Ibrahim, L. C. Abdullah and T. C. Ping, *Journal of Nano Research*, 2010, 10, 29-37.
100. N. Kanipandian, S. Kannan, R. Ramesh, P. Subramanian and R. Thirumurugan, *Mater. Res. Bull.*, 2014, 49, 494-502.
101. S. S. Shankar, A. Ahmad and M. Sastry, *Biotechnol. Progr.*, 2003, 19, 1627-1631.
102. J. Liu, D. A. Sonshine, S. Shervani and R. H. Hurt, *ACS Nano*, 2010, 4, 6903-6913.
103. D. Huang, B. Ou and R. L. Prior, *J. Agric. Food. Chem.*, 2005, 53, 1841-1856.

104. H. Ikigai, T. Nakae, Y. Hara and T. Shimamura, *Biochim. Biophys. Acta*, 1993, 1147, 132-136.
105. Y. Cui, Y. J. Oh, J. Lim, M. Youn, I. Lee, H. K. Pak, W. Park, W. Jo and S. Park, *Food Microbiol.*, 2012, 29, 80-87.
106. Y. Yoda, Z.-Q. Hu, T. Shimamura and W.-H. Zhao, *J. Infect. Chemother.*, 2004, 10, 55-58.
107. N. Sahiner, *Materials Science and Engineering: C*, 2014, 44, 9-16.
108. N. Sahiner, S. Sagbas and N. Aktas, *Materials Science and Engineering: C*, 2015, 49, 824-834.
109. P. R. Judzewitsch, T.-K. Nguyen, S. Shanmugam, E. H. H. Wong and C. A. J. M. Boyer, *Angew. Chem. Int. Ed.*, DOI: 10.1002/anie.201713036.
110. T. Y. Kim, S.-H. Cha, S. Cho and Y. Park, *Arch. Pharmacol Res.*, 2016, 39, 465-473.
111. S. Siddhartha, B. Tanmay, R. Arnab, S. Gajendra, P. Ramachandrarao and D. Debabrata, *Nanotechnology*, 2007, 18, 225103.
112. S. Agnihotri, S. Mukherji and S. Mukherji, *RSC Advances*, 2014, 4, 3974-3983.
113. C. Willyard, *Nature*, 2017, 543.
114. C.-N. Lok, C.-M. Ho, R. Chen, Q.-Y. He, W.-Y. Yu, H. Sun, P. K.-H. Tam, J.-F. Chiu and C.-M. Che, *JBIC Journal of Biological Inorganic Chemistry*, 2007, 12, 527-534.
115. A. M. E. Badawy, T. P. Luxton, R. G. Silva, K. G. Scheckel, M. T. Suidan and T. M. Tolaymat, *Environ. Sci. Technol.*, 2010, 44, 1260-1266.
116. D. P. Gnanadhas, M. Ben Thomas, R. Thomas, A. M. Raichur and D. Chakravortty, *Antimicrob. Agents Chemother.*, 2013, 57, 4945-4955.
117. E. Amato, Y. A. Diaz-Fernandez, A. Taglietti, P. Pallavicini, L. Pasotti, L. Cucca, C. Milanese, P. Grisoli, C. Dacarro, J. M. Fernandez-Hechavarria and V. Necchi, *Langmuir*, 2011, 27, 9165-9173.
118. L. Kvítek, A. Panáček, J. Soukupová, M. Kolář, R. Večeřová, R. Pucek, M. Holecová and R. Zbořil, *The Journal of Physical Chemistry C*, 2008, 112, 5825-5834.
119. R. Namivandi-Zangeneh, R. J. Kwan, T.-K. Nguyen, J. Yeow, F. L. Byrne, S. H. Oehlers, E. H. H. Wong and C. Boyer, *Polymer Chemistry*, 2018, DOI: 10.1039/C7PY01069A.
120. Z. Sadrearhami, J. Yeow, T.-K. Nguyen, K. K. K. Ho, N. Kumar and C. Boyer, *Chem. Commun.*, 2017, 53, 12894-12897.
121. O. M. Vandeputte, M. Kiendrebeogo, S. Rajaonson, B. Diallo, A. Mol, M. El Jaziri and M. Baucher, *Appl. Environ. Microbiol.*, 2010, 76, 243-253.
122. A. M. Königs, H.-C. Flemming and J. Wingender, *Front. Microbiol.*, 2015, 6.